HHS Public Access

Author manuscript

Trends Cancer. Author manuscript; available in PMC 2019 May 01.

Published in final edited form as:

Trends Cancer. 2018 May ; 4(5): 359–373. doi:10.1016/j.trecan.2018.03.009.

Noninvasive PET Imaging of T cells

Weijun Wei[1,2,5], **Dawei Jiang**[2,5], **Emily B. Ehlerding**[3], **Quanyong Luo**[1,*], and **Weibo Cai**[2,3,4,*]

[1]Department of Nuclear Medicine, Shanghai Jiao Tong University Affiliated Sixth People's Hospital, Shanghai 200233, China

[2]Department of Radiology, Department of Medical Physics, University of Wisconsin, Madison, WI 53705, USA

[3]Department of Medical Physics, University of Wisconsin, Madison, WI 53705, USA

[4]University of Wisconsin Carbone Cancer Center, Madison, Wisconsin 53705, USA

Abstract

The rapidly evolving field of cancer immunotherapy recently saw the approval of several new therapeutic antibodies. Several cell therapies, for example, chimeric antigen receptor-expressing T cells (CAR-T), are currently in clinical trials for a variety of cancers and other diseases. However, approaches to monitor changes in the immune status of tumors or to predict therapeutic responses are limited. Monitoring lymphocytes from whole blood or biopsies does not provide dynamic and spatial information about T cells in heterogeneous tumors. Positron emission tomography (PET) imaging using probes specific for T cells can noninvasively monitor systemic and intratumoral immune alterations during experimental therapies and may have an important and expanding value in the clinic.

PET Imaging of T Cells in the Era of Cancer Immunotherapy and Personalized Medicine

The field of immuno-oncology expanded rapidly in the past decade, with the approval of several immune checkpoint targeting antibodies and cell-based therapies, like adoptive cell transfer (ACT) [1,2]. Immune checkpoints, such as the programmed cell death protein 1 (PD-1), its ligand (programmed cell death protein ligand 1, PD-L1), and cytotoxic T lymphocyte antigen 4 (CTLA-4), provide immune-inhibitory signals in the tumor microenvironment, and inhibitors of CTLA-4, PD-1, or PD-L1 have resulted in durable tumor regression in some patients [3]. While immune checkpoint inhibitors rely on the development of functional antitumor T cells to mediate cancer regression *in vivo*, ACT is a highly personalized cancer therapy option in which large numbers of antitumor lymphocytes can be prepared either by extracting tumor-infiltrating lymphocytes (TILs) or from genetic engineering of lymphocytes *in vitro* [2]. Traditional ACT mainly relies on cloning T cell receptors (TCRs) and genetically engineering these TCRs into the peripheral blood lymphocytes (PBLs) of appropriate patients. Another approach uses a novel chimeric

*Correspondence: lqyn@sh163.net (Q. Luo) and wcai@uwhealth.org (W. Cai).

[5]These authors contributed equally to this work

antigen receptor (CAR) composed of a ligand-binding domain, which was derived from the single chain variable fragment (scFv) of a monoclonal antibody (mAb) to enable tumor-specific binding, and a transmembrane domain that activates T cells [1]. More recent CAR-T techniques aim to develop mutation-reactive TILs targeting tumor-specific mutated proteins, and it has been suggested that CAR-Ts targeting cancer neoantigens may represent the 'final common pathway' which will result in cancer regression [4].

Immunotherapy revolutionized the clinical treatment of certain cancers, such as melanoma [5,6], non-small cell lung cancer (NSCLC) [7,8], advanced lymphoma [9,10], and liquid B cell tumors [11]. Although immune checkpoint inhibitors and T cell therapies are rapidly evolving treatment modalities, only a subgroup of patients respond and many patients experience side effects associated with these new therapies. Therefore, monitoring and visualizing immune responses longitudinally could be of great importance to better stratify patients and select responders during the course of immunotherapy [12]. Indeed, analysis of TILs may help with predicting therapeutic outcome and survival in melanoma, urogenital, lung, ovarian, and colorectal cancers [13–15], and with stratifying patients in clinical trials [16,17]. Immune responses are commonly assessed by measuring levels of circulating lymphocytes, cytokines, and immunoglobulins in blood samples, or by biopsies of tumor tissue, spleen, and lymph nodes. These methods are invasive and cannot provide comprehensive information of the entire tumor mass and metastases, yielding poorly reliable data to correlate the immune cell infiltration status with the outcome of immunotherapies. In addition, morphological assessments used in solid tumors [i.e., response evaluation criteria in solid tumors (RECIST)] are not reliable in evaluating early tumor response to biological therapies [18]. In this setting, development of T cell-targeting, noninvasive imaging probes is of clinical importance and may facilitate better management of cancer patients following immunotherapies.

Noninvasive methods for tracking T cells are mainly based on direct cell labeling, radiolabeling of intact antibodies or antibody fragments, metabolism-based tracers, and reporter gene-based tracers [19]. *In vitro* direct or indirect labeling of immune cells employs fluorescent agents, bioluminescent agents, magnetic resonance imaging (MRI) contrast agents, or radiolabeled probes such as ^{18}F-fluorodeoxyglucose (^{18}F-FDG). However, T cell tracking strategies based on labeling have inherent limitations, such as potential toxicity to the therapeutic cells, dilution of imaging agents upon cell death, and restricted longitudinal imaging, which may limit their clinical translation [20–22]. In comparison, T cell-specific probes prepared by labeling antibodies or small molecules harbor great translational potential and some of them have entered clinical trials. The imaging modalities applied for T cell imaging include optical imaging, MRI, single photon emission computed tomography (SPECT), and positron emission tomography (PET). While optical cell-tracking methods have distinct advantages in preclinical small animal models, they are not optimal for human whole-body scans, since the detectability of this modality is limited by its poor tissue penetration. PET imaging has high sensitivity and tissue penetration and is suitable for tracking T cells in both preclinical animal models and in clinical settings [23,24]. In conjunction with various cell-tracking methods, PET imaging can quantify the number of viable T cells and their retention in tumors, which may provide insight into therapeutic responses. In areas other than oncology, substantial studies have also explored and validated

the utility of T cell imaging techniques in detecting several immune-related conditions, such as graft-versus-host disease (GVHD) [25], inflammatory bowel diseases (IBD) [26], hematopoietic stem cell transplantation (HSCT) [27], and tuberculosis [28]. We herein review the most recent developments in PET imaging techniques for visualizing T cells and emphasize potential clinical applications (Figure 1 and Table 1).

Protein/Peptide-Based T Cell Imaging

In immunoPET tracking of cytotoxic T cells (CTLs), radiolabeled antibodies or antibody-derived constructs target general T cell markers such as CD3, CD4, and CD8, or immune checkpoints like PD-1, PD-L1, or CTLA-4. Apart from monoclonal antibodies, single-domain antibodies (sdAbs) and glycoprotein-targeting interleukins have been also harnessed to track T cells.

Intact Antibodies

CTLA-4 is a transmembrane inhibitory receptor expressed on activated T lymphocytes. Interaction of CD80/CD86 and CTLA-4 causes inhibition of T cell activation through several mechanisms that include raising the T cell activation threshold and attenuating clonal expansion. Blockade of CTLA-4 with ipilimumab or tremelimumab limits the CD80/CD86-CTLA-4 interaction and shows clinical anticancer efficacy [29]. PET imaging has recently been used to determine the levels of PD-1/PD-L1 positive or CTLA-4-positive tissues in preclinical models (reviewed in [30]). Higashikawa and colleagues developed a CTLA-4-targeting PET probe (^{64}Cu-DOTA-anti-CTLA-4 mAb) using an anti-mouse CTLA-4 mAb, and found that the probe accumulated significantly more in CT26 tumor-bearing BALB/c mice when compared with cultured CT26 cells or in CT26 tumor-bearing nude mice. These results suggested that tumor-infiltrating T cells were responsible for the high CTLA-4 expression [31]. Ehlerding *et al.* have recently developed a ^{64}Cu-DOTA-ipilimumab probe that showed enhanced and persistent accumulation in CTLA-4-expressing lung cancer models, indicating that certain tumor cells express CTLA-4 and ^{64}Cu-DOTA-ipilimumab may guide CTLA-4 targeted therapies in the future [32]. Since the study by Ehlerding *et al.* showed specific binding of ^{64}Cu-DOTA-ipilimumab to tumor tissues, future studies are still needed to determine whether the signal from CTLA-4^{+} TILs can be separated from tracer binding to tumor cells. CD3 is a global T lymphocyte marker and may potentially serve as an abundant marker to monitor immunotherapy responses. Larimer *et al.* developed ^{89}Zr-DFO-CD3 to help predict immune response to therapy with CTLA-4 checkpoint inhibitors [33]. After anti-CTLA-4 treatment of CT26 tumor-bearing mice, PET imaging using ^{89}Zr-DFO-CD3 delineated murine colon carcinomas. More importantly, higher uptake of the radiotracer (which indicated an increased presence of CD3^{+} TILs) correlated with smaller tumor volumes [33]. This study showed that PET imaging of CD3^{+} T cell infiltration may represent a useful and noninvasive imaging option to predict tumor responses to CTLA-4 blockade before anatomic changes become apparent.

PD-1 on T cells interacts with PD-L1 and this interaction in the tumor microenvironment plays a major role in the suppression of T cell responses [34]. Blockade of the PD-1/PD-L1 pathway is a highly promising therapeutic strategy and has elicited durable antitumor

responses in a broad spectrum of cancers [35]. Initial attempts to image T cells by targeting PD-1 used mAbs against murine PD-1. Natarajan *et al.* developed a PD-1 targeting PET probe using a murine mAb and suggested that PD-1 targeted PET imaging may have potential to assess the prognostic value of PD-1 in preclinical models of immunotherapy, but this tool is limited to image the expression of murine PD-1 [36]. Nivolumab is a human mAb targeting PD-1, a negative regulator of T cell activation and response. England *et al.* have synthesized a ^{89}Zr-Df-nivolumab probe that maps the localization of PD-1-expressing TILs *in vivo* in humanized murine models of lung cancer (Figure 2A) [37]. Cole *et al.* studied the biodistribution of ^{89}Zr-Df-nivolumab in healthy non-human primates, and reported that the probe was primarily cleared through liver and high uptake in the spleen could be reduced by administration of excess unlabeled nivolumab [38]. Initial clinical studies showed that ^{89}Zr-Df-nivolumab PET was a safe and feasible method to map PD-1 expression [39]. Pembrolizumab, a humanized IgG4 monoclonal anti-PD-1 antibody, is approved for the treatment of advanced melanoma, NSCLC, head and neck squamous cell cancer, classical Hodgkin lymphoma, advanced urothelial cancer, advanced gastric cancer, and microsatellite instability-high cancers [40]. We recently developed a ^{89}Zr-labeled pembrolizumab probe that enabled dynamic tracking of T cell checkpoint receptor expression, and measured the biodistribution and pharmacokinetics of pembrolizumab *in vivo* [41]. Since this initial report, ^{89}Zr-pembrolizumab was further assessed in humanized A375 melanoma-bearing mouse models by Natarajan *et al.* [42], and the same team developed ^{64}Cu-pembrolizumab, reporting the utility of this probe in delineating PD-1-expressing T lymphocytes in preclinical mouse models [43]. Other PD-1 and PD-L1 targeted immunoPET probes (^{64}Cu-NOTA-PD-1 and ^{64}Cu-NOTA-PD-L1), developed by Hettich *et al.* [44], enabled the specific detection of the spleen and individual lymph nodes after IFN-γ injection. Notably, ^{64}Cu-NOTA-PD-1 detected PD-1^{+} TILs after combined γ-irradiation and immunotherapy in melanoma models, since radiotherapy can strongly upregulate TILs [44–46]. ^{64}Cu-NOTA-PD-L1 PET could also serve as an important tool in exploring mechanisms involved with PD-L1-mediated immune escape [47]. These studies demonstrate the potential clinical value of immune checkpoint PET imaging in the assessment of T cell dynamics, cancer diagnostics, and patient stratification, before starting immunotherapy.

Single-Domain Antibodies and Antibody Fragments

Compared with intact antibodies, sdAbs and antibody fragments have superior imaging characteristics, such as rapid clearance, high target-to-background ratios, reduced radiation dose, and engineered sites for site-specific conjugation [48–51]. Generally, sdAbs can be produced from camelid heavy-chain-only IgGs (VHHs), from cartilaginous fish IgNARs (VNARs), or from human IgGs [52,53]. Human sdAbs can be selected from human antibodies or humanized from camelid sdAbs [54,55], and contain the variable domain of the heavy chain (VH) or light chain (VL). Substantial preclinical data has shown that sdAb-based molecular imaging is promising and may play an important role in the diagnosis of various diseases (reviewed in [48]). Initial studies showed that radiolabeled VHHs could be used to image inflammation in both xenogeneic and syngeneic tumor models [56]. More recently, Rashidian *et al.* developed a VHH specific for CD8 and labeled the antibody with ^{89}Zr after polyethylene glycol (PEG) modification. One of the synthesized probes, ^{89}Zr-PEG20-X118-VHH, specifically visualized lymphoid organs such as the spleen and lymph

nodes [57]. This probe also visualized melanoma and pancreatic cancers by detecting tumor-infiltrating lymphocytes, and distinguished therapy responsive versus nonresponsive tumors through longitudinal immunoPET monitoring of $CD8^+$ TILs [57]. Van Elssen *et al.* developed a radiolabeled VHH (^{64}Cu-labeled VHH4) that recognizes HLA-DR (human class II MHC products expressed on antigen-presenting cells, activated T cells, and natural killer cells), and reported that PET imaging using this probe detected inflammation (presence of activated human T cells) in xenograft models of chronic GVHD. In particular, BLT mice (developed by reconstituting NSG mice with human fetal thymus, liver, and liver-derived hematopoietic stem cells) with GVHD had a higher uptake of the tracer in the liver when compared with normal BLT mice (Figure 2B), which was caused by increased human T cell infiltration [25]. Together, these studies indicate that it is possible to image human immune responses noninvasively with VHH-based PET imaging.

Solid evidence suggests that an increased presence of $CD4^+$ and $CD8^+$ lymphocytes in the tumor microenvironment is predictive of improved prognosis and response to immunomodulatory therapy [17,58]. Tavaré *et al.* initially showed the feasibility of engineering minibody (Mb) fragments from anti-murine CD8-depleting antibodies (clones 2.43 and YTS169.4.2.1), and found that immunoPET imaging using either ^{64}Cu-NOTA-2.43 Mb or ^{64}Cu-NOTA-YTS169 Mb identified $CD8^+$ positive organs (spleen, lymph nodes, and liver) *in vivo*. Furthermore, ^{64}Cu-NOTA-2.43 Mb only detected $CD8^+$ positive organs in C57BL/6 (B/6) mice, but not in CD8 blocking B6 mice or in B6 mice which had received anti-CD8 antibody depletion therapy (Figure 2C) [59]. The same team then engineered a specific probe, ^{89}Zr-malDFO-169, which detected tumor-infiltrating $CD8^+$ T cells in mouse models after antigen-specific adoptive T cell transfer, anti-CD137, or anti-PD-L1 immunotherapy [60]. These studies therefore indicate the feasibility of anti-CD8 immunoPET imaging in reflecting both systemic and intratumoral alterations of the $CD8^+$ T cells following different models of immunotherapy. Intact antibodies can also be engineered into bivalent antibody fragments, and cys-diabodies (cDb) are one such platform with enhanced immunoPET imaging characteristics [49]. ^{89}Zr-malDFO-GK1.5 cDb and ^{89}Zr-malDFO-2.43 cDb, two other PET probes developed by Tavaré *et al.* [27], are two promising probes for detecting $CD4^+$ T cells and $CD8^+$ T cells, respectively. ^{89}Zr-malDFO-GK1.5 cDb and ^{89}Zr-malDFO-2.43 cDb immunoPET are robust methods for monitoring *in vivo* lymphocyte dynamics in preclinical models of HSCT [27,61]. As $CD4^+$ T cells are known mediators of inflammation in IBD [62], immunoPET using ^{89}Zr-malDFO-GK1.5 cDb can also serve a useful antibody-based imaging method in studying $CD4^+$ T cells in IBD models [26]. An ongoing Phase I clinical trial (NCT03107663) also aims to evaluate the safety and imaging ability of ^{89}Zr-Df-IAB22M2C [63], an anti-CD8 minibody radiolabeled with ^{89}Zr, for imaging human $CD8^+$ T cells in patients with selected solid tumors.

Peptides and Interleukins

The very late antigen-4 (VLA-4, also called integrin $\alpha_4\beta_1$) is a heterodimer of integrins expressed at the surface of inflammatory cells and tumor cells [64,65]. LLP2A, a high-affinity 495 peptidomimetic ligand for VLA-4, has been used in preclinical imaging studies of primary and metastatic melanoma [66,67]. Mattila *et al.* demonstrated that the ^{64}Cu-LLP2A probe bound to macrophages and T cells in granulomas [28]. In complete Freund's

adjuvant (CFA)-induced murine inflammation models, ^{64}Cu-LLP2A, rather than ^{18}F-FDG, concentrated in metabolically active inflammatory cells as early as 2 h postinjection. In macaque tuberculosis models, the uptake of ^{64}Cu-LLP2A in granulomas was higher than in uninfected tissues, and significant correlations between the LLP2A signal and macrophage and T cell numbers were observed (Figure 2D) [28]. These results indicate that ^{64}Cu-LLP2A, when used in conjunction with ^{18}F-FDG, may serve as a useful tool to study granulomas in inflammation and tuberculosis.

Granzyme B is a serine protease that activates caspases. It is released by $CD8^+$ T cells and natural killer cells during immune responses and is one of the two dominant mechanisms by which T cells mediate cancer cell death [68]. Larimer *et al.* developed a peptide inhibitor of granzyme B and then used it to create a PET probe, ^{68}Ga-NOTA-GZP, which was capable of detecting the release of murine granzyme B by actively engaged immune cells [69]. ^{68}Ga-NOTA-GZP predicted responses to anti-PD-1 and anti-CTLA-4 combination immunotherapy in colon cancer models [69]. In this study, the authors also developed a humanized version of GZP, and performed immunohistochemical analyses of human melanoma biopsy samples from nine patients treated with anti-PD-1 checkpoint inhibitors. The authors found that, when compared with treatment responders, nonresponders had higher granzyme B expression, suggesting the potential value of ^{68}Ga-NOTA-GZP PET to specifically distinguish responsive and nonresponsive patients with melanoma before anti-PD-1 immunotherapy [69].

High levels of interleukin-2 receptors (IL-2R) are present at the surface of activated $CD4^+$ and $CD8^+$ T lymphocytes [70], and high-dose IL-2 treatment shows efficacy in patients with metastatic melanoma and renal cancer [71]. Studies have been dedicated to imaging activated T lymphocytes via labeling of IL-2 with various isotopes for both SPECT and PET [72,73]. Based on previous studies reporting that PET with [^{18}F]FB-IL2 accurately quantified lymphocytic infiltration [74], de Vries *et al.* showed a 10- and 27-fold higher uptake of [^{18}F]FB-IL-2 in lung tumor-bearing mice receiving tumor irradiation alone or in combination with immunization over untreated controls [75], suggesting that the probe can serve as a noninvasive imaging tool for monitoring activated T lymphocytes in the context of local tumor treatments. More recently, a mutant of IL2 (IL2v) with abolished CD25 binding, increased plasma half-life, and less toxicity [76], was radiolabeled using fluorine-18 and assessed in preclinical mouse models [51]. When compared with [^{18}F]FB-IL2, [^{18}F]FB-IL2v had slower plasma kinetics, therefore indicating that mutant IL2v could be superb either as a therapeutic drug or as a molecular imaging agent [77].

Metabolism-Based T Cell Imaging

PET probes targeting metabolic pathways, such as ^{18}F-FDG and ^{18}F-FLT (^{18}F-fluorothymidine) can potentially monitor diverse cell types involved in innate and adaptive immunity [78]. ^{18}F-FDG is the most commonly used PET tracer. Transport of ^{18}F-FDG is mainly mediated by a Na^+-dependent glucose transporter (GLUT). Increased uptake of ^{18}F-FDG has been found in various cancers due to overexpression of GLUT isotypes and overproduction of hexokinase enzyme; however, inflammatory cells and granulation tissues may exhibit similar metabolism of ^{18}F-FDG due to their increased expression of GLUT

isotypes (mainly GLUT-1 and GLUT-3) after cytokine or mutagen stimulation [79]. ^{18}F-FDG PET has been used to evaluate inflammation and to monitor the efficacy of immunotherapy [80,81]. Still, there is a notable rate of false-positive signals in the context of immune cell detection and glycolysis in both cancerous and noncancerous diseases. ^{18}F-FLT is taken up by proliferating cells and phosphorylated by thymidine kinase 1 (TK), leading to intracellular trapping of the tracer, which therefore reflects cellular TK activity and cellular proliferation [82]. Two decades ago, Shields *et al.* demonstrated that ^{18}F-FLT could be concentrated by submandibular lymph nodes and non-Hodgkin's lymphoma in dog models [83]. In recent years, ^{18}F-FLT PET has been increasingly used to image tumor proliferation in clinical practice [84,85], and to monitor lymphocyte activation after treatment with dendritic cell-based vaccines in clinical settings [86]. Considering the nonspecific properties of ^{18}F-FDG and ^{18}F-FLT PET, PET imaging using probes that can measure distinct functional parameters of immune cells *in vivo* could substantially facilitate better evaluation of cancer immunotherapy.

Although most tissues predominantly utilize *de novo* DNA synthesis, lymphoid organs and rapidly proliferating tissues alternatively rely on salvage pathways [87]. Deoxycytidine kinase (dCK) is a rate-limiting enzyme in the deoxyribonucleoside salvage pathway, important for the production and maintenance of a balanced pool of deoxyribonucleoside triphosphates (dNTPs). Therefore, there has been a focus on designing PET probes using fluorinated dCK substrates to image T cells. [^{18}F]FAC {1-(2′-deoxy-2′-[^{18}F]fluoroarabinofuranosyl) cytosine}, a nucleoside analog radiotracer discovered by screening the retention of [^{3}H]-labeled deoxyribonucleoside analogs in resting versus proliferating primary CD8^{+} T cells [88], has selective specificity for lymphoid organs [89]. Radu *et al.* demonstrated that [^{18}F]FAC enabled visualization of lymphoid organs and localization of immune activation in a mouse model of antitumor immunity, whereas ^{18}F-FDG preferentially accumulated in tumor lesions [88]. These two agents may thus provide complimentary information: FAC for T cell infiltration and FDG for tumor cells themselves.

Since rapid catabolism of [^{18}F]FAC, mediated by cytidine deaminase (CDA), may limit its clinical utility [89], and dCK phosphorylates both pyrimidines and purines [90], Kim *et al.* developed a purine [^{18}F]CFA (2-chloro-2′-deoxy-2′-[^{18}F]fluoro-9-β-D-arabinofuranosyl-adenine) which was validated as a primary substrate for cytosolic dCK and is resistant to CDA-mediated deamination. A first-in-human study using [^{18}F]CFA showed that the probe significantly accumulated in dCK-positive tissues (bone marrow, liver, and spleen) and in the axillary lymph nodes (Figure 3A) [91]. The high specificity of [^{18}F]CFA for dCK and its corresponding favorable biodistribution in humans justify further studies to validate [^{18}F]CFA PET as a new cancer biomarker and to investigate the potential utility of this probe in assessing immunological diseases. In a recent clinical study assessing the therapeutic efficacy of PD-1 blockade in glioblastoma (GBM) patients, Antonios *et al.* determined that, unlike the rapid catabolism of the first dCK PET probe [^{18}F]-FAC by CDA in humans, the accumulation of[^{18}F]-FAC was significantly enhanced in tumors and secondary lymphoid organs after PD-1 immunotherapy using pembrolizumab, and intratumoral [^{18}F]-FAC uptake was correlated to the concentration of tumor-associated T lymphocytes [92]. MRI may provide better anatomic resolution than PET in detecting brain tumors, so in this study the authors determined that a combination of [^{18}F]-CFA PET and

advanced MRI may be useful for differentiating tumor progression from immune cell infiltration [92]. Indeed, contrast-enhanced MRI (CE-MRI) is the most sensitive and reproducible method available to measure brain metastases and assess response to treatment [93]. However, it does not differentiate tumor progression from pseudoprogression, or immune inflammatory responses from other sources of contrast enhancement on MRI. These proof-of-concept studies strongly indicate that [^{18}F]-CFA PET, when used alone or in combination with CE-MRI, could provide fundamental functional information by selectively discriminating immune responses.

Arabinosyl guanine (AraG) is a compound with specific toxicity to T lymphocyte and T lymphoblastoid cells. Nelarabine, a water-soluble AraG prodrug, has been used to treat patients with refractory or relapsed T cell acute lymphoblastic leukemia and T cell lymphoblastic lymphoma [94]. The striking immune selectivity of this drug led to the development of a [^{18}F]F-AraG probe, and initial results showed that [^{18}F]F-AraG is retained by primary T cells [95]. This led to [^{18}F]F-AraG PET/CT images with an apparent increase in tracer accumulation in the cervical lymph nodes in acute GVHD models compared with controls, in concert with higher total body luminescence signal from luciferase-positive donor T cells (Figure 3B) [96,97]. Therefore, [^{18}F]F-AraG PET imaging may be useful to detect T cell dynamics, or to monitor new immunosuppressive therapies. Indeed, Franc *et al.* recently demonstrated that [^{18}F]F-AraG PET may serve as an imaging biomarker of T cell activation for rheumatoid arthritis [98].

Reporter Gene-Based T Cell Imaging Techniques

Reporter gene imaging, whereby cells are transfected with a PET reporter gene that encodes a protein specifically targeted via a radiolabeled reporter probe, has been used to image ACTs and CAR-Ts [99–101].

The herpes simplex virus type 1 thymidine kinase (*HSV1-tk*) is under extensive study as a PET reporter gene to image gene expression in both preclinical animal models and clinical subjects (note: *HSV1-tk* refers to the gene while HSV1-TK refers to the corresponding enzyme) [102]. Substrates of HSV1-TK are pyrimidine nucleoside derivatives or acycloguanosine derivatives [103]. A mutant reporter gene, *HSV1-sr39tk*, with improved affinity for acycloguanosine and decreased affinity for the native substrate thymidine, has also been reported [104]. Studies comparing different reporter probes showed that a radiolabeled acycloguanosine derivative probe ([^{18}F]FHBG) was more sensitive than the pyrimidine nucleoside radiolabeled probe ([^{14}C] FIAU) in the *HSV1-sr39tk* system [105]. Thunemann *et al.* recently showed that longitudinal [^{18}F] FHBG-PET imaging quantified T cell homing during inflammation and cardiomyocyte viability after myocardial infarction [106]. Different human-derived reporter systems for potential T cell tracking, such as the human sodium iodide symporter (hNIS)/^{124}I-iodide, and the human norepinephrine transporter (hNET)/^{123}I/^{124}I-metaiodobenzylguanidine (MIBG) have also been investigated [101].

A cornerstone in field is the [^{18}F]FHBG/*HSV1-tk* PET imaging system developed by Yaghoubi *et al.* [107,108]. In a pilot clinical study, the authors expanded autologous CD8^{+}

CTLs which were genetically modified to express the CAR IL-13 zetakine gene, *HSV1-tk* suicide gene, and PET imaging reporter gene. After injection into the tumor resection site of a high-grade GBM patient, these engineered T cells specifically targeted tumor cells in an IL-13 zetakine-dependent manner and allowed molecular PET imaging because these T cells expressed HSV1-TK enzyme which mediated [^{18}F]FHBG uptake [108]. The value of [^{18}F]FHBG in longitudinal monitoring of the trafficking, survival, and proliferation of CTLs was confirmed in seven patients with recurrent high-grade GBMs, resistant to conventional therapies [109]. Given that the nonspecific retention of [^{18}F]FHBG in previous surgical sites or in brain parenchyma may affect the interpretation of the maximum standardized uptake value (SUV_{max}), the authors derived volumes of interest (VOI) by comparing CE-MRI taken before and after CTL infusions, and then calculated total activity by using a new imaging metric (defined as $SUV_{mean} \times$ VOI) before and after CTL infusions. Qualitative assessment of [^{18}F]FHBG uptake on pre- and post-CTL injection PET scans revealed an increase in PET signal after CTL infusions, which indicates CTL cell trafficking and viability (Figure 3C). In patients where the size of the VOI or SUV_{mean} did not change, the total activity of [^{18}F]FHBG increased after CTL infusions [109].

Mall *et al.* proposed a highly sensitive imaging strategy to track TCR-transduced human T cells *in vivo* by directly targeting the TCR2.5D6 (TCR2.5D6 is a TCR that recognizes a myeloperoxidase-derived HLA peptide expressed on leukemia cells, as described previously [110]) with a ^{89}Zr-aTCRmu-F(ab′)$_2$ probe. Animals treated with TCR2.5D6-transduced human CD8$^+$ central memory T cells had a distinct signal at the tumor site in comparison with controls. This imaging technology, but not ^{18}F-FDG PET, was able to map the differential distribution of T cell infiltration within the tumor, and thereby reflected T cell dynamics after intravenous injection of central memory T cells [111]. ^{89}Zr-aTCRmu-F(ab·)$_2$ also detected signals of as little as 1.0×10^4 T cells in more clinically relevant models [112]. These preclinical results highlight the value of developing PET-guided adoptive T cell therapy using TCR-transgenic T cells.

Concluding Remarks

We presented here the most recent developments in PET imaging techniques to visualize T cells. These noninvasive methods may have considerable impact in the diagnosis and evaluation of treatment in various malignancies and immunological disorders. These imaging strategies can also monitor the viability, biodistribution, and trafficking of therapeutic cells to tumor sites. Clinical translation of some of these promising probes may facilitate optimal management of cancer patients.

As we and others have previously reviewed [30,48,113,114], molecular imaging can provide nearly real-time information about target and receptor expression levels in the era of cancer immunotherapy [115–118], and PET imaging can provide a powerful means to measure biological changes such as metabolism, cell location, and tumor burden [119]. T cell tracking systems that combine T cell-specific probes with highly sensitive PET imaging also allow longitudinal PET imaging and quantification of T cell dynamics. Besides its value for basic research, tracking T cells noninvasively *in vivo* can facilitate individualized medicine

and accelerate the development of new diagnostic tools and clinical therapeutic strategies [30,120].

The use of mAbs for cancer immunotherapy has rapidly expanded during the past 10 years, and a number of promising radiolabeled mAbs have been used to target T cells [121,122]. However, mAbs have a molecular weight of ~150 kDa, dimensions of 14.2 × 8.5 × 3.8 nm [123], and 'binding site barriers' [124], which may limit their distribution and penetration into tumors. In addition, mAbs typically have several days of half-life in the bloodstream, which for PET imaging may result in high background levels. Naturally derived or synthetic antigen-binding fragments, Fv, and scFv have smaller sizes [125], but lower affinities and limited stability, which may limit clinical translation. Nanobodies, which are specifically heavy chain-only antibodies from camelid species [53,55], have sufficient antigen binding properties and are considered as powerful candidates for *in vivo* T cell tracking and molecular imaging [48,50]. More recently, adnectins, a family of engineered proteins with smaller sizes (~10 kDa) [126], have been used to design a PD-L1-targeting PET probe (^{18}F-BMS-986192) [127], and clinical trials in patients with NSCLC demonstrated the feasibility and safety of noninvasive PET imaging of PD-L1 status in tumors using this probe [39]. Future studies may use these candidates to develop T cell-specific PET probes with improved *in vivo* performance. Besides the imaging quality of antibody/nanobody based PET probes for T cell tracing, an important concern is their potential to induce immunogenic responses. Therefore, PET probes based on FDA-approved antibodies may find their way to the clinic for molecular imaging of T cells in the coming future, as these have already been thoroughly tested [30]. For other promising probes illustrated in this review, substantial preclinical studies and refinement strategies (such as complete humanization or chimerization of proteins) are needed to avoid unwanted immune responses in patients. Immunodeficient mice reconstituted with a human immune system, such as hu-PBL-NSG mice (NSG mice reconstituted with human PBLs) used in our group [37,41], or other humanized mice used by other groups [25,128,129], are valuable tools to experimentally manipulate human cells *in vivo* and facilitate the development of better probes.

To date, several PET radiotracers based on T cell metabolism have been developed for imaging the immune system and even specific cell types such as activated T cells. This provides the impetus for clinical evaluation of some of these very promising probes for cancer in the era of immunotherapy and for other immune-mediated inflammatory diseases such as GVHD and tuberculosis. Besides its role in detecting dynamics of T cells, future studies may also investigate the potential utility of [^{18}F]F-AraG PET in gastrointestinal stromal tumors, because [^{18}F]F-AraG PET imaging in healthy human volunteers resulted in low background in the thorax and gastrointestinal tract [96], and dysregulated nucleoside metabolism represents a hallmark of cancer [130]. In addition, most of these small molecule probes exhibited rapid blood clearance, so they can be labeled with short and intermediate half-life radioisotopes such as ^{18}F.

Noninvasive PET imaging based on reporter gene strategies enables imaging over the entire lifetime of a cell, and provides information on cell viability since the signal is maintained with cell division [131]. Reporter gene imaging could allow longitudinal tracking of T cells, but relies on the *ex vivo* transfection of cells and, for clinical translation, the development of

nonimmunogenic PET reporter proteins is a prerequisite [132]. Gaps related to the distribution and persistence of the genetically altered cells, identified by their resistance to neomycin or hygromycin toxicity, need to be thoroughly investigated before clinical translation. The [^{18}F] FHBG/CAR-T theranostic system has shown promise for the treatment of high-grade gliomas in humans; however, CTL infusion techniques allowing efficient and tumor-site-specific delivery of CTLs are yet to be optimized. As CTLs that express *HSV1-tk* undergo ganciclovir-induced programmed cell death, future studies may explore strategies that prolong the survival of engineered CTLs and improve their therapeutic efficacy, in turn improving imaging sensitivity. In addition, pre- and postinfusion [^{18}F]FHBG PET scanning together with MRI may facilitate more accurate measurement of CTL delivery and nonspecific retention of the radiotracer [109].

To conclude, over the past decade, robust PET imaging approaches have been established to noninvasively image T cells. Still, many questions remain regarding the feasibility, safety, and specificity of these T cell imaging techniques in the clinical setting (see Outstanding Questions).

Acknowledgments

This work was sponsored by the PhD Innovation Fund of Shanghai Jiao Tong University School of Medicine (No. BXJ201736), the Shanghai Key Discipline of Medical Imaging (No. 2017ZZ02005), the University of Wisconsin, Madison, the National Institutes of Health (P30CA014520, T32CA009206, and T32GM008505) and the American Cancer Society (125246-RSG-13-099-01-CCE). Weijun Wei was partially funded by the China Scholarship Council (CSC).

References

1. Yang JC, Rosenberg SA. Adoptive T-cell therapy for cancer. Adv. Immunol. 2016; 130:279–294. [PubMed: 26923004]
2. Rosenberg SA, Restifo NP. Adoptive cell transfer as personalized immunotherapy for human cancer. Science. 2015; 348:62–68. [PubMed: 25838374]
3. Mahoney KM, et al. Combination cancer immunotherapy and new immunomodulatory targets. Nat. Rev. Drug Discov. 2015; 14:561–584. [PubMed: 26228759]
4. Tran E, et al. ‘Final common pathway’ of human cancer immunotherapy: targeting random somatic mutations. Nat. Immunol. 2017; 18:255–262. [PubMed: 28198830]
5. Morgan RA, et al. Cancer regression in patients after transfer of genetically engineered lymphocytes. Science. 2006; 314:126–129. [PubMed: 16946036]
6. Heppt MV, et al. Immune checkpoint blockade for unresectable or metastatic uveal melanoma: a systematic review. Cancer Treat Rev. 2017; 60:44–52. [PubMed: 28881222]
7. Tabchi S, et al. Management of stage III non-small cell lung cancer. Semin. Oncol. 2017; 44:163–177. [PubMed: 29248128]
8. Antonia SJ, et al. Durvalumab after chemoradiotherapy in stage III non-small-cell lung cancer. N. Engl. J. Med. 2017; 377:1919–1929. [PubMed: 28885881]
9. Kochenderfer JN, et al. Eradication of B-lineage cells and regression of lymphoma in a patient treated with autologous T cells genetically engineered to recognize CD19. Blood. 2010; 116:4099–4102. [PubMed: 20668228]
10. Brudno JN, Kochenderfer JN. Chimeric antigen receptor T-cell therapies for lymphoma. Nat. Rev. Clin. Oncol. 2018; 15:31–46. [PubMed: 28857075]
11. Kalos M, et al. T cells with chimeric antigen receptors have potent antitumor effects and can establish memory in patients with advanced leukemia. Sci. Transl. Med. 2011; 3:95ra73.

12. Kraeber-Bodere F, et al. ImmunoPET to help stratify patients for targeted therapies and to improve drug development. Eur. J. Nucl. Med. Mol. Imaging. 2016; 43:2166–2168. [PubMed: 27539021]
13. Pages F, et al. Immune infiltration in human tumors: a prognostic factor that should not be ignored. Oncogene. 2010; 29:1093–1102. [PubMed: 19946335]
14. Solinas C, et al. The immune infiltrate in prostate, bladder and testicular tumors: an old friend for new challenges. Cancer Treat. Rev. 2017; 53:138–145. [PubMed: 28113097]
15. Wei SC, et al. Distinct cellular mechanisms underlie anti-CTLA-4 and anti-PD-1 checkpoint blockade. Cell. 2017; 170:1120–1133. [PubMed: 28803728]
16. Dieci, MV., et al. Update on tumor-infiltrating lymphocytes (TILs) in breast cancer, including recommendations to assess TILs in residual disease after neoadjuvant therapy and in carcinoma *in situ*: a report of the International Immuno-Oncology Biomarker Working Group on Breast Cancer. Semin. Cancer Biol. 2017. Published online October 9, 2017. http://dx.doi.org/10.1016/j.semcancer.2017.10.003
17. Smyth MJ, et al. Combination cancer immunotherapies tailored to the tumour microenvironment. Nat. Rev. Clin. Oncol. 2016; 13:143–158. [PubMed: 26598942]
18. Rossi S, et al. Clinical characteristics of patient selection and imaging predictors of outcome in solid tumors treated with checkpoint-inhibitors. Eur. J. Nucl. Med. Mol. Imaging. 2017; 44:2310–2325. [PubMed: 28815334]
19. Liu Z, Li Z. Molecular imaging in tracking tumor-specific cytotoxic T lymphocytes (CTLs). Theranostics. 2014; 4:990–1001. [PubMed: 25157278]
20. Matsui K, et al. Quantitation and visualization of tumor-specific T cells in the secondary lymphoid organs during and after tumor elimination by PET. Nucl. Med. Biol. 2004; 31:1021–1031. [PubMed: 15607484]
21. Pittet MJ, et al. *In vivo* imaging of T cell delivery to tumors after adoptive transfer therapy. Proc. Natl. Acad. Sci. U. S. A. 2007; 104:12457–12461. [PubMed: 17640914]
22. Botti C, et al. Comparison of three different methods for radiolabelling human activated T lymphocytes. Eur. J. Nucl. Med. 1997; 24:497–504. [PubMed: 9142729]
23. Dobrenkov K, et al. Monitoring the efficacy of adoptively transferred prostate cancer-targeted human T lymphocytes with PET and bioluminescence imaging. J. Nucl. Med. 2008; 49:1162–1170. [PubMed: 18552144]
24. Yaghoubi S, et al. Human pharmacokinetic and dosimetry studies of [(18)F]FHBG: a reporter probe for imaging herpes simplex virus type-1 thymidine kinase reporter gene expression. J. Nucl. Med. 2001; 42:1225–1234. [PubMed: 11483684]
25. Van Elssen C, et al. Noninvasive imaging of human immune responses in a human xenograft model of graft-versus-host disease. J. Nucl. Med. 2017; 58:1003–1008. [PubMed: 28209904]
26. Freise, AC., et al. ImmunoPET in inflammatory bowel disease: imaging $CD4^+$ T cells in a murine model of colitis. J. Nucl. Med. 2018. Published online January 11, 2018. http://dx.doi.org/10.2967/jnumed.117.199075
27. Tavaré R, et al. Immuno-PET of murine T cell reconstitution postadoptive stem cell transplantation using anti-CD4 and anti-CD8 cys-diabodies. J. Nucl. Med. 2015; 56:1258–1264. [PubMed: 25952734]
28. Mattila JT, et al. Positron emission tomography imaging of macaques with tuberculosis identifies temporal changes in granuloma glucose metabolism and integrin alpha4beta1-expressing immune cells. J. Immunol. 2017; 199:806–815. [PubMed: 28592427]
29. Boutros C, et al. Safety profiles of anti-CTLA-4 and anti-PD-1 antibodies alone and in combination. Nat. Rev. Clin. Oncol. 2016; 13:473–486. [PubMed: 27141885]
30. Ehlerding EB, et al. Molecular imaging of immunotherapy targets in cancer. J. Nucl. Med. 2016; 57:1487–1492. [PubMed: 27469363]
31. Higashikawa K, et al. ^{64}Cu-DOTA-anti-CTLA-4 mAb enabled PET visualization of CTLA-4 on the T-cell infiltrating tumor tissues. PLoS One. 2014; 9:e109866. [PubMed: 25365349]
32. Ehlerding EB, et al. ImmunoPET imaging of CTLA-4 expression in mouse models of non-small cell lung cancer. Mol. Pharm. 2017; 14:1782–1789. [PubMed: 28388076]
33. Larimer BM, et al. Quantitative CD3 PET imaging predicts tumor growth response to anti-CTLA-4 therapy. J. Nucl. Med. 2016; 57:1607–1611. [PubMed: 27230929]

34. Chen L, Han X. Anti-PD-1/PD-L1 therapy of human cancer: past, present, and future. J. Clin. Invest. 2015; 125:3384–3391. [PubMed: 26325035]
35. Zou W, et al. PD-L1 (B7-H1) and PD-1 pathway blockade for cancer therapy: mechanisms, response biomarkers, and combinations. Sci. Transl. Med. 2016; 8:328rv4.
36. Natarajan A, et al. Novel radiotracer for immunoPET imaging of PD-1 checkpoint expression on tumor infiltrating lymphocytes. Bioconjug. Chem. 2015; 26:2062–2069. [PubMed: 26307602]
37. England CG, et al. (89)Zr-labeled nivolumab for imaging of T-cell infiltration in a humanized murine model of lung cancer. Eur. J. Nucl. Med. Mol. Imaging. 2018; 45:110–120. [PubMed: 28821924]
38. Cole EL, et al. Radiosynthesis and preclinical PET evaluation of (89)Zr-nivolumab (BMS-936558) in healthy non-human primates. Bioorg. Med. Chem. 2017; 25:5407–5414. [PubMed: 28803798]
39. Niemeijer A-LN, et al. Whole body PD-1 and PD-L1 PET with ^{89}Zr-nivolumab and ^{18}F-BMS-986192 in pts with NSCLC. J. Clin. Oncol. 2017; 35(15):e20047.
40. Peters S, et al. PD-1 blockade in advanced NSCLC: a focus on pembrolizumab. Cancer Treat. Rev. 2018; 62:39–49. [PubMed: 29156447]
41. England CG, et al. Preclinical pharmacokinetics and biodistribution studies of ^{89}Zr-labeled pembrolizumab. J. Nucl. Med. 2017; 58:162–168. [PubMed: 27493273]
42. Natarajan A, et al. Development of novel immunoPET tracers to image human PD-1 checkpoint expression on tumor-infiltrating lymphocytes in a humanized mouse model. Mol. Imaging Biol. 2017; 19:903–914. [PubMed: 28247187]
43. Natarajan A, et al. Dosimetry prediction for clinical translation of (64)Cu-pembrolizumab immunoPET targeting human PD-1 expression. Sci. Rep. 2018; 8:633. [PubMed: 29330552]
44. Hettich M, et al. High-resolution PET imaging with therapeutic antibody-based PD-1/PD-L1 checkpoint tracers. Theranostics. 2016; 6:1629–1640. [PubMed: 27446497]
45. Deng L, et al. From DNA damage to nucleic acid sensing: a strategy to enhance radiation therapy. Clin. Cancer Res. 2016; 22:20–25. [PubMed: 26362999]
46. Ngwa, W., et al. Using immunotherapy to boost the abscopal effect. Nat. Rev. Cancer. 2018. Published online February 16, 2018. http://dx.doi.org/10.1038/nrc.2018.6
47. Prestipino A, et al. Oncogenic JAK2(V617F) causes PD-L1 expression, mediating immune escape in myeloproliferative neoplasms. Sci. Transl. Med. 2018; 10:eaam7729. [PubMed: 29467301]
48. Chakravarty R, et al. Nanobody: the “magic bullet” for molecular imaging? Theranostics. 2014; 4:386–398. [PubMed: 24578722]
49. Wu AM. Engineered antibodies for molecular imaging of cancer. Methods. 2014; 65:139–147. [PubMed: 24091005]
50. Oliveira S, et al. Targeting tumors with nanobodies for cancer imaging and therapy. J. Control Rel. 2013; 172:607–617.
51. Warnders FJ, et al. Biodistribution and PET imaging of labeled bispecific T cell-engaging antibody targeting EpCAM. J. Nucl. Med. 2016; 57:812–817. [PubMed: 26848172]
52. Boldicke T. Single domain antibodies for the knockdown of cytosolic and nuclear proteins. Protein Sci. 2017; 26:925–945. [PubMed: 28271570]
53. Pardon E, et al. A general protocol for the generation of nanobodies for structural biology. Nat. Protoc. 2014; 9:674–693. [PubMed: 24577359]
54. Vincke C, et al. General strategy to humanize a camelid single-domain antibody and identification of a universal humanized nanobody scaffold. J. Biol. Chem. 2009; 284:3273–3284. [PubMed: 19010777]
55. Ingram, JR., et al. Exploiting nanobodies’ singular traits. Annu. Rev. Immunol. 2018. Published online February 28, 2018. http://dx.doi.org/10.1146/annurev-immunol-042617-053327
56. Rashidian M, et al. Noninvasive imaging of immune responses. Proc. Natl. Acad. Sci. U. S. A. 2015; 112:6146–6151. [PubMed: 25902531]
57. Rashidian M, et al. Predicting the response to CTLA-4 blockade by longitudinal noninvasive monitoring of CD8 T cells. J. Exp. Med. 2017; 214:2243–2255. [PubMed: 28666979]
58. Jiang W, et al. Immune priming of the tumor microenvironment by radiation. Trends Cancer. 2016; 2:638–645. [PubMed: 28741502]

59. Tavaré R, et al. Engineered antibody fragments for immuno-PET imaging of endogenous $CD8^+$ T cells *in vivo*. Proc. Natl. Acad. Sci. U. S. A. 2014; 111:1108–1113. [PubMed: 24390540]
60. Tavaré R, et al. An effective immuno-PET imaging method to monitor CD8-dependent responses to immunotherapy. Cancer Res. 2016; 76:73–82. [PubMed: 26573799]
61. Freise AC, et al. ImmunoPET imaging of murine CD4(+) T cells using anti-CD4 cys-biabody: effects of protein dose on T cell function and imaging. Mol. Imaging Biol. 2017; 19:599–609. [PubMed: 27966069]
62. Geremia A, et al. Innate and adaptive immunity in inflammatory bowel disease. Autoimmun. Rev. 2014; 13:3–10. [PubMed: 23774107]
63. Olafsen T, et al. Pet imaging of cytotoxic human T cells using an ^{89}Zr-labeled anti-CD8 minibody. J. Immunother. Cancer. 2015; 3:P388.
64. Schlesinger M, Bendas G. Contribution of very late antigen-4 (VLA-4) integrin to cancer progression and metastasis. Cancer Metastasis Rev. 2015; 34:575–591. [PubMed: 25564456]
65. Wei W, et al. PET and SPECT imaging of melanoma: the state of the art. Eur. J. Nucl. Med. Mol. Imaging. 2018; 45:132–150. [PubMed: 29085965]
66. Beaino W, Anderson CJ. PET imaging of very late antigen-4 in melanoma: comparison of ^{68}Ga- and ^{64}Cu-labeled NODAGA and CB-TE1A1P-LLP2A conjugates. J. Nucl. Med. 2014; 55:1856–1863. [PubMed: 25256059]
67. Beaino W, et al. Evaluation of (68)Ga- and (177)Lu-DOTA-PEG4-LLP2A for VLA-4-targeted PET imaging and treatment of metastatic melanoma. Mol. Pharm. 2015; 12:1929–1938. [PubMed: 25919487]
68. Nagata S. Apoptosis by death factor. Cell. 1997; 88:355–365. [PubMed: 9039262]
69. Larimer BM, et al. Granzyme B PET imaging as a predictive biomarker of immunotherapy response. Cancer Res. 2017; 77:2318–2327. [PubMed: 28461564]
70. Malek TR, Castro I. Interleukin-2 receptor signaling: at the interface between tolerance and immunity. Immunity. 2010; 33:153–165. [PubMed: 20732639]
71. Rosenberg SA. IL-2: the first effective immunotherapy for human cancer. J. Immunol. 2014; 192:5451–5458. [PubMed: 24907378]
72. Signore A, et al. 123I-interleukin-2 scintigraphy for *in vivo* assessment of intestinal mononuclear cell infiltration in Crohn's disease. J. Nucl. Med. 2000; 41:242–249. [PubMed: 10688106]
73. Di Gialleonardo V, et al. N-(4-^{18}F-fluorobenzoyl)interleukin-2 for PET of human-activated T lymphocytes. J. Nucl. Med. 2012; 53:679–686. [PubMed: 22499614]
74. Di Gialleonardo V, et al. Pharmacokinetic modelling of N-(4-[(18)F]fluorobenzoyl)interleukin-2 binding to activated lymphocytes in an xenograft model of inflammation. Eur. J. Nucl. Med. Mol. Imaging. 2012; 39:1551–1560. [PubMed: 22777334]
75. Hartimath SV, et al. Noninvasive monitoring of cancer therapy induced activated T cells using [^{18}F]FB-IL-2 PET imaging. Oncoimmunology. 2017; 6:e1248014. [PubMed: 28197364]
76. Klein C, et al. Cergutuzumab amunaleukin (CEA-IL2v), a CEA-targeted IL-2 variant-based immunocytokine for combination cancer immunotherapy: overcoming limitations of aldesleukin and conventional IL-2-based immunocytokines. Oncoimmunology. 2017; 6:e1277306. [PubMed: 28405498]
77. Hartimath SV, et al. Pharmacokinetic properties of radiolabeled mutant Interleukin-2v: a PET imaging study. Oncotarget. 2018; 9:7162–7174. [PubMed: 29467958]
78. Laing RE, et al. Visualizing cancer and immune cell function with metabolic positron emission tomography. Curr. Opin. Genet. Dev. 2010; 20:100–105. [PubMed: 19931447]
79. Meller J, et al. ^{18}F-FDG PET and PET/CT in fever of unknown origin. J. Nucl. Med. 2007; 48:35–45. [PubMed: 17204697]
80. Wong ANM, et al. The advantages and challenges of using FDG PET/CT for response assessment in melanoma in the era of targeted agents and immunotherapy. Eur. J. Nucl. Med. Mol. Imaging. 2017; 44(Suppl. 1):67–77. [PubMed: 28389693]
81. Seith F, et al. ^{18}F-FDG-PET detects complete response to PD1-therapy in melanoma patients two weeks after therapy start. Eur. J. Nucl. Med. Mol. Imaging. 2018; 45:95–101. [PubMed: 28831583]

82. Tehrani OS, Shields AF. PET imaging of proliferation with pyrimidines. J. Nucl. Med. 2013; 54:903–912. [PubMed: 23674576]
83. Shields AF, et al. Imaging proliferation *in vivo* with [F-18] FLT and positron emission tomography. Nat. Med. 1998; 4:1334–1336. [PubMed: 9809561]
84. Schelhaas S, et al. Preclinical applications of 30′-deoxy-30′-[(18)F]fluorothymidine in oncology – a systematic review. Theranostics. 2017; 7:40–50. [PubMed: 28042315]
85. Ribas A, et al. Imaging of CTLA4 blockade-induced cell replication with (18)F-FLT PET in patients with advanced melanoma treated with tremelimumab. J. Nucl. Med. 2010; 51:340–346. [PubMed: 20150263]
86. Aarntzen EH, et al. Early identification of antigen-specific immune responses *in vivo* by [^{18}F]-labeled 30′-fluoro-30′-deoxythymidine ([^{18}F]FLT) PET imaging. Proc. Natl. Acad. Sci. U. S. A. 2011; 108:18396–18399. [PubMed: 22025695]
87. Griffith DA, Jarvis SM. Nucleoside and nucleobase transport systems of mammalian cells. Biochim. Biophys. Acta. 1996; 1286:153–181. [PubMed: 8982282]
88. Radu CG, et al. Molecular imaging of lymphoid organs and immune activation by positron emission tomography with a new [^{18}F]-labeled 2′-deoxycytidine analog. Nat. Med. 2008; 14:783–788. [PubMed: 18542051]
89. Schwarzenberg J, et al. Human biodistribution and radiation dosimetry of novel PET probes targeting the deoxyribonucleoside salvage pathway. Eur. J. Nucl. Med. Mol. Imaging. 2011; 38:711–721. [PubMed: 21127859]
90. Arner ES, Eriksson S. Mammalian deoxyribonucleoside kinases. Pharmacol. Ther. 1995; 67:155–186. [PubMed: 7494863]
91. Kim W, et al. [^{18}F]CFA as a clinically translatable probe for PET imaging of deoxycytidine kinase activity. Proc. Natl. Acad. Sci. U. S. A. 2016; 113:4027–4032. [PubMed: 27035974]
92. Antonios JP, et al. Detection of immune responses after immunotherapy in glioblastoma using PET and MRI. Proc. Natl. Acad. Sci. U. S. A. 2017; 114:10220–10225. [PubMed: 28874539]
93. Lin NU, et al. Response assessment criteria for brain metastases: proposal from the RANO group. Lancet Oncol. 2015; 16:e270–e278. [PubMed: 26065612]
94. Roecker AM, et al. Nelarabine in the treatment of refractory T-cell malignancies. Clin. Med. Insights Oncol. 2010; 4:133–141. [PubMed: 21151585]
95. Namavari M, et al. Synthesis of 2′-deoxy-2′-[^{18}F]fluoro-9-beta-D-arabinofuranosylguanine: a novel agent for imaging T-cell activation with PET. Mol. Imaging Biol. 2011; 13:812–818. [PubMed: 20838911]
96. Ronald JA, et al. A PET imaging strategy to visualize activated T cells in acute graft-versus-host disease elicited by allogenic hematopoietic cell transplant. Cancer Res. 2017; 77:2893–2902. [PubMed: 28572504]
97. Beilhack A, et al. Prevention of acute graft-versus-host disease by blocking T-cell entry to secondary lymphoid organs. Blood. 2008; 111:2919–2928. [PubMed: 17989315]
98. Franc BL, et al. *In vivo* PET imaging of the activated immune environment in a small animal model of inflammatory arthritis. Mol. Imagin. 2017; 16 1536012117712638.
99. Nair-Gill ED, et al. Non-invasive imaging of adaptive immunity using positron emission tomography. Immunol. Rev. 2008; 221:214–228. [PubMed: 18275485]
100. Koya RC, et al. Kinetic phases of distribution and tumor targeting by T cell receptor engineered lymphocytes inducing robust antitumor responses. Proc. Natl. Acad. Sci. U. S. A. 2010; 107:14286–14291. [PubMed: 20624956]
101. Moroz MA, et al. Comparative analysis of T cell imaging with human nuclear reporter genes. J. Nucl. Med. 2015; 56:1055–1060. [PubMed: 26025962]
102. Najjar AM, et al. Imaging of sleeping beauty-modified CD19-specific T cells expressing HSV1-thymidine kinase by positron emission tomography. Mol. Imaging Biol. 2016; 18:838–848. [PubMed: 27246312]
103. Gambhir SS, et al. Imaging transgene expression with radionuclide imaging technologies. Neoplasia. 2000; 2:118–138. [PubMed: 10933072]

104. Gambhir SS, et al. A mutant herpes simplex virus type 1 thymidine kinase reporter gene shows improved sensitivity for imaging reporter gene expression with positron emission tomography. Proc. Natl. Acad. Sci. U. S. A. 2000; 97:2785–2790. [PubMed: 10716999]
105. Min JJ, et al. Comparison of [^{18}F]FHBG and [^{14}C]FIAU for imaging of HSV1-tk reporter gene expression: adenoviral infection vs stable transfection. Eur. J. Nucl. Med. Mol. Imaging. 2003; 30:1547–1560. [PubMed: 14579096]
106. Thunemann M, et al. Cre/lox-assisted non-invasive *in vivo* tracking of specific cell populations by positron emission tomography. Nat. Commun. 2017; 8:444. [PubMed: 28874662]
107. Yaghoubi SS, Gambhir SS. PET imaging of herpes simplex virus type 1 thymidine kinase (HSV1-tk) or mutant HSV1-sr39tk reporter gene expression in mice and humans using [^{18}F]FHBG. Nat. Protoc. 2006; 1:3069–3075. [PubMed: 17406570]
108. Yaghoubi SS, et al. Noninvasive detection of therapeutic cytolytic T cells with ^{18}F-FHBG PET in a patient with glioma. Nat. Clin. Pract. Oncol. 2009; 6:53–58. [PubMed: 19015650]
109. Keu KV, et al. Reporter gene imaging of targeted T cell immunotherapy in recurrent glioma. Sci. Transl. Med. 2017; 9:eaag2196. [PubMed: 28100832]
110. Klar R, et al. Therapeutic targeting of naturally presented myeloperoxidase-derived HLA peptide ligands on myeloid leukemia cells by TCR-transgenic T cells. Leukemia. 2014; 28:2355–2366. [PubMed: 24736212]
111. Mall S, et al. Immuno-PET imaging of engineered human T cells in tumors. Cancer Res. 2016; 76:4113–4123. [PubMed: 27354381]
112. Yusufi N, et al. In-depth characterization of a TCR-specific tracer for sensitive detection of tumor-directed transgenic T cells by immuno-PET. Theranostics. 2017; 7:2402–2416. [PubMed: 28744323]
113. Evangelista L, et al. The new era of cancer immunotherapy: what can molecular imaging do to help? Clin. Transl. Imaging. 2017; 5:299–301. [PubMed: 29181372]
114. McCracken MN, et al. Advances in PET detection of the antitumor T cell response. Adv. Immunol. 2016; 131:187–231. [PubMed: 27235684]
115. Byun DJ, et al. Cancer immunotherapy – immune checkpoint blockade and associated endocrinopathies. Nat. Rev. Endocrinol. 2017; 13:195–207. [PubMed: 28106152]
116. Francis DM, Thomas SN. Progress and opportunities for enhancing the delivery and efficacy of checkpoint inhibitors for cancer immunotherapy. Adv. Drug Deliv. Rev. 2017; 114:33–42. [PubMed: 28455187]
117. Goel S, et al. Positron emission tomography and nanotechnology: a dynamic duo for cancer theranostics. Adv. Drug Deliv. Rev. 2017; 113:157–176. [PubMed: 27521055]
118. Sun H, et al. ImmunoPET for assessing the differential uptake of a CD146-specific monoclonal antibody in lung cancer. Eur. J. Nucl. Med. Mol. Imaging. 2016; 43:2169–2179. [PubMed: 27342417]
119. James ML, Gambhir SS. A molecular imaging primer: modalities, imaging agents, and applications. Physiol. Rev. 2012; 92:897–965. [PubMed: 22535898]
120. Kircher MF, et al. Noninvasive cell-tracking methods. Nat. Rev. Clin. Oncol. 2011; 8:677–688. [PubMed: 21946842]
121. Pardoll DM. The blockade of immune checkpoints in cancer immunotherapy. Nat. Rev. Cancer. 2012; 12:252–264. [PubMed: 22437870]
122. Topalian SL, et al. Mechanism-driven biomarkers to guide immune checkpoint blockade in cancer therapy. Nat. Rev. Cancer. 2016; 16:275–287. [PubMed: 27079802]
123. Sarma VR, et al. The three-dimensional structure at 6 A resolution of a human gamma Gl immunoglobulin molecule. J. Biol. Chem. 1971; 246:3753–3759. [PubMed: 5578919]
124. Fujimori K, et al. A modeling analysis of monoclonal antibody percolation through tumors: a binding-site barrier. J. Nucl. Med. 1990; 31:1191–1198. [PubMed: 2362198]
125. Yap ML, et al. Targeting activated platelets: a unique and potentially universal approach for cancer imaging. Theranostics. 2017; 7:2565–2574. [PubMed: 28819447]
126. Sha F, et al. Monobodies and other synthetic binding proteins for expanding protein science. Protein Sci. 2017; 26:910–924. [PubMed: 28249355]

127. Donnelly DJ, et al. Synthesis and biologic evaluation of a novel (18)F-labeled adnectin as a PET radioligand for imaging PD-L1 expression. J. Nucl. Med. 2018; 59:529–535. [PubMed: 29025984]

128. Brainard DM, et al. Induction of robust cellular and humoral virus-specific adaptive immune responses in human immunodeficiency virus-infected humanized BLT mice. J. Virol. 2009; 83:7305–7321. [PubMed: 19420076]

129. Greenblatt MB, et al. Graft versus host disease in the bone marrow, liver and thymus humanized mouse model. PLoS One. 2012; 7:e44664. [PubMed: 22957096]

130. Hanahan D, Weinberg RA. Hallmarks of cancer: the next generation. Cell. 2011; 144:646–674. [PubMed: 21376230]

131. Kurtz DM, Gambhir SS. Tracking cellular and immune therapies in cancer. Adv. Cancer Res. 2014; 124:257–296. [PubMed: 25287692]

132. Yaghoubi SS, et al. Positron emission tomography reporter genes and reporter probes: gene and cell therapy applications. Theranostics. 2012; 2:374–391. [PubMed: 22509201]

Highlights

Positron emission tomography (PET) imaging is a noninvasive and reproducible diagnostic technology for optimizing therapeutic strategies.

T cell-specific PET imaging can visualize tumor-infiltrating lymphocytes and monitor the dynamics of T cells in response to chemotherapy, radiotherapy, molecularly targeted therapy, immunotherapy, and adoptive cell transfer.

ImmunoPET imaging gives information on the *in vivo* behavior of therapeutic monoclonal antibodies (i.e., tumor targeting, quantitative variation in molecular targets, and accumulation of monoclonal antibodies in critical normal organs) and, as a result, may optimize clinical management for patients who receive immune checkpoint inhibitor treatment.

ImmunoPET tracers using nanobodies or antibody fragments and short-lived PET radionuclides may enhance the target-to-background ratio and reduce radiation dose.

Reporter gene-based T cell imaging techniques can be used to noninvasively monitor fate of therapeutic T cells *in vivo* and therefore to refine infusion strategies.

Clinical application of PET imaging of T cell dynamics is not limited to visualizing T cells in the tumor microenvironment, but could also extend to detect inflammatory diseases.

Outstanding Questions

Substantial preclinical PET studies have validated the utility of detecting T cell-specific markers in the tumor microenvironment (both lineage markers and immune checkpoints), but to what extent will these imaging technologies be translated and how will they guide clinical decisions?

While many immune checkpoint receptors and ligands have been discovered, not all of these molecules are solely expressed by T cells. Are there other, extremely T cell-specific markers that can be employed for designing imaging probes?

One concern when designing T cell-specific PET probes is the overlap in metabolism of T cells located in lymph nodes and intratumorally. Are there any highly specific metabolites that can be used and radiolabeled to trace tumor-infiltrating lymphocytes? Are there any metabolites highly enriched in tumor-infiltrating lymphocytes but not in tumor cells?

Enzymatic PET reporter genes have been widely explored to track T cells. Will induced expression of a foreign protein trigger immune responses, or cause malignant transformation to transfected cells?

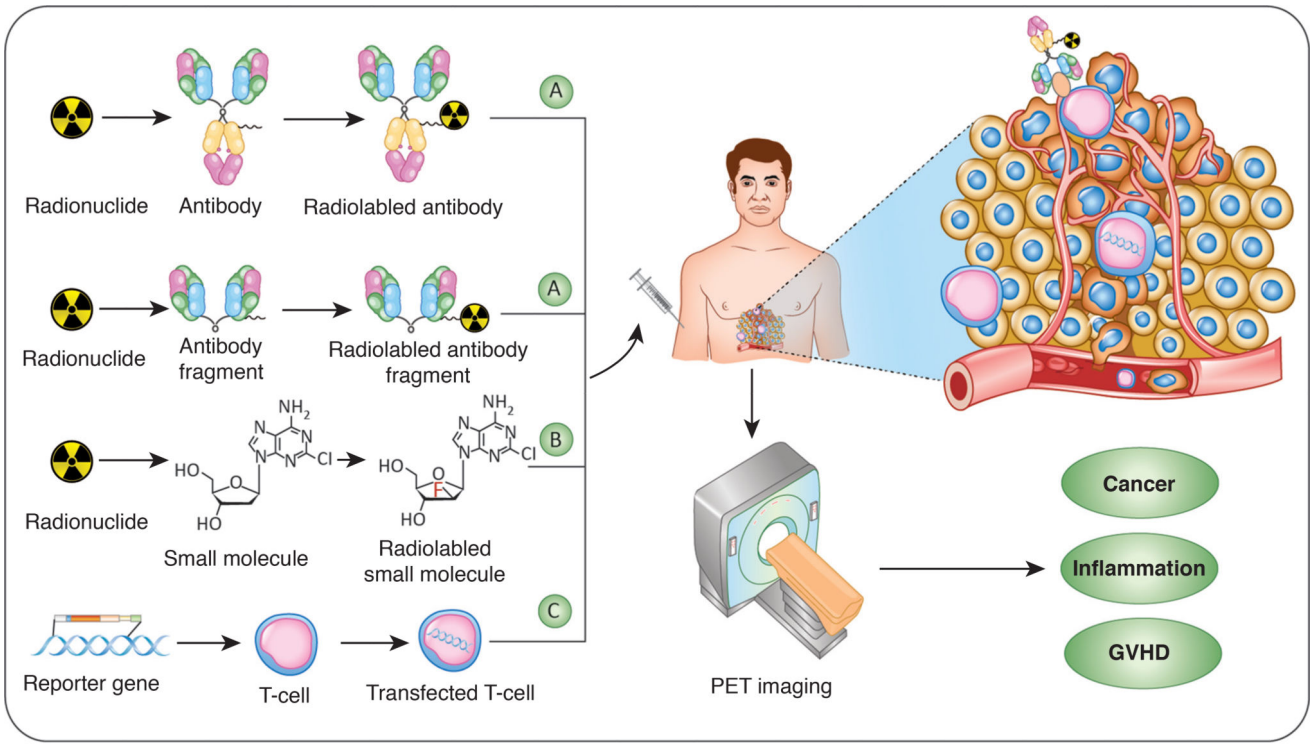

Figure 1. Strategies for Positron Emission Tomography (PET) Imaging of T cells

Noninvasive PET imaging of T cells can be used for cancer diagnostics, disease monitoring, and patient stratification. Furthermore, the application of these imaging techniques can also be extended to evaluate inflammatory diseases, such as rheumatoid arthritis and graft-versus-hostdisease (GVHD). (A) Targeting extracellular epitopes at the surface of T cells *in vivo* with highly specific antibodies or antibody fragments enables noninvasive PET imaging of T cells. Short-lived or long-lived PET radionuclides can be used to label T cell-specific antibodies/antibody fragments/proteins. (B) Small molecules and metabolites can be modified or directly radiolabeled to track T cells. [^{18}F]CFA displayed in the figure is a typical representative probe. (C) PET imaging with reporter genes requires genetic modification of T cells. The T cells are transfected with a vector which contains a promoter that regulates the expression of a reporter gene (may encode receptors, fluorescent proteins, or enzymes), which activates the injected imaging probe or mediates its accumulation in T cells.

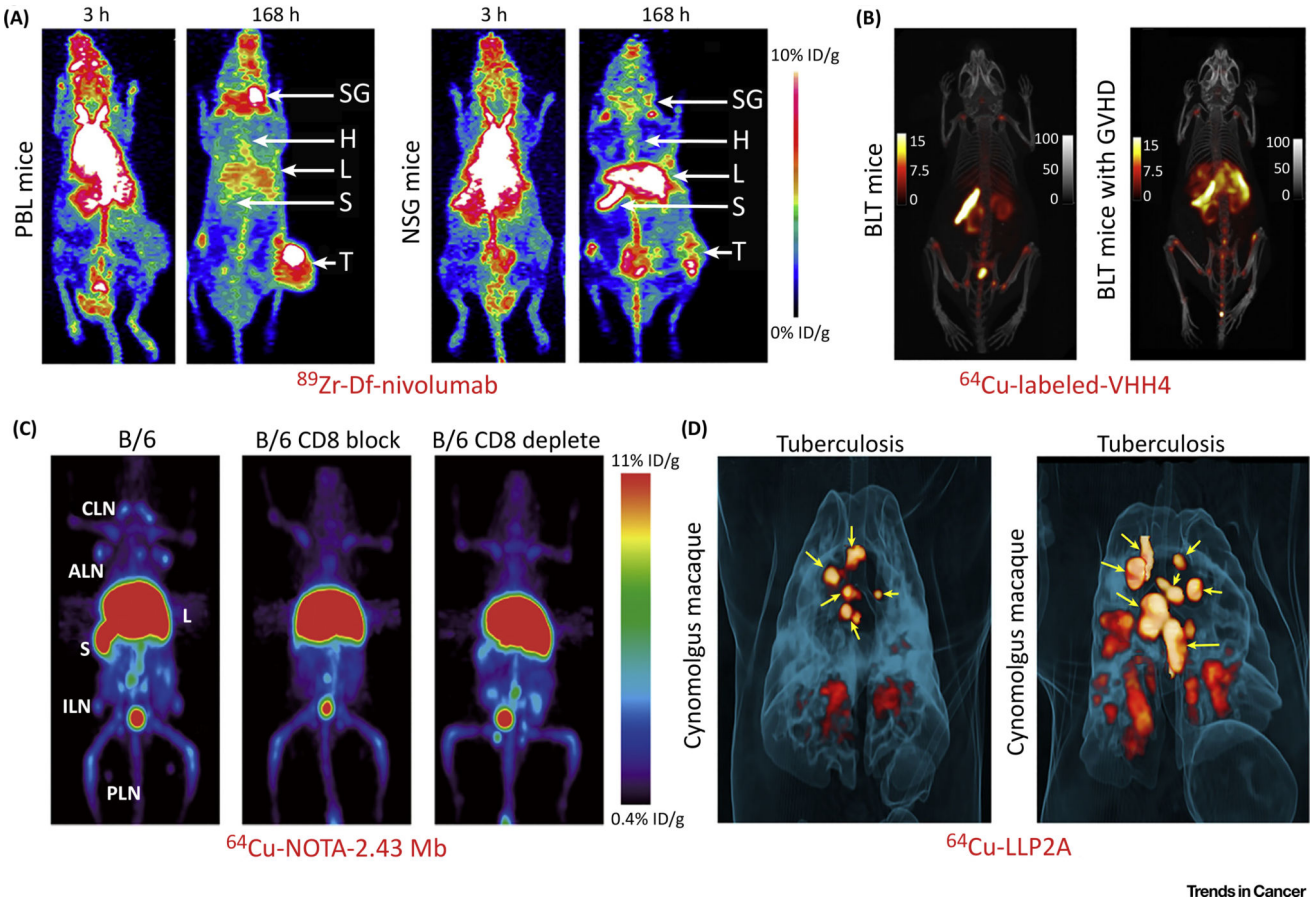

Figure 2. Positron Emission Tomography (PET) Imaging with Labeled Antibodies, Antibody Fragments, or Proteins Detects T Cells

(A) ^{89}Zr-Df-nivolumab successfully maps the *in vivo* biodistribution of tumor-infiltrating T cells expressing PD-1 in tumor-bearing mice. Note that tumor uptake of the tracer was much higher in humanized PBL tumor-bearing mice (left) than that in NSG tumor-bearing mice (right), which indicated infiltration of tumor-infiltrating lymphocytes into the tumor microenvironment in PBL mice. (B) ^{64}Cu-labeled VHH4 PET imaging of BLT mice (left) and BLT mice with stage 3 graft-versus-host disease (GVHD) (right). The results showed that BLT mice with GVHD had intense PET signal in the liver, which indicated T cell infiltration in the affected liver. (C) ImmunoPET imaging of T cells using ^{64}Cu-NOTA-2.43 minibody (Mb) in antigen-blocked and antigen-depleted B/6 mice. (D) ^{64}Cu-LLP2A PET imaging of cynomolgus macaques infected with the *Mycobacterium tuberculosis* strain Erdman. Maximum intensity projections showed that ^{64}Cu-LLP2A uptake in granulomas and infected lymph nodes before necropsy. Yellow arrows indicate lymph nodes. Adapted, with permission, from [28,37,57,60]. Abbreviations: ALN, axillary lymph nodes; B, bone; B/6, C57BL/6; CLN, cervical lymph nodes; H, heart; ILN, inguinal lymph nodes; L, liver; PLN, popliteal lymph nodes; S, spleen; SG, salivary gland; T, A549 tumor.

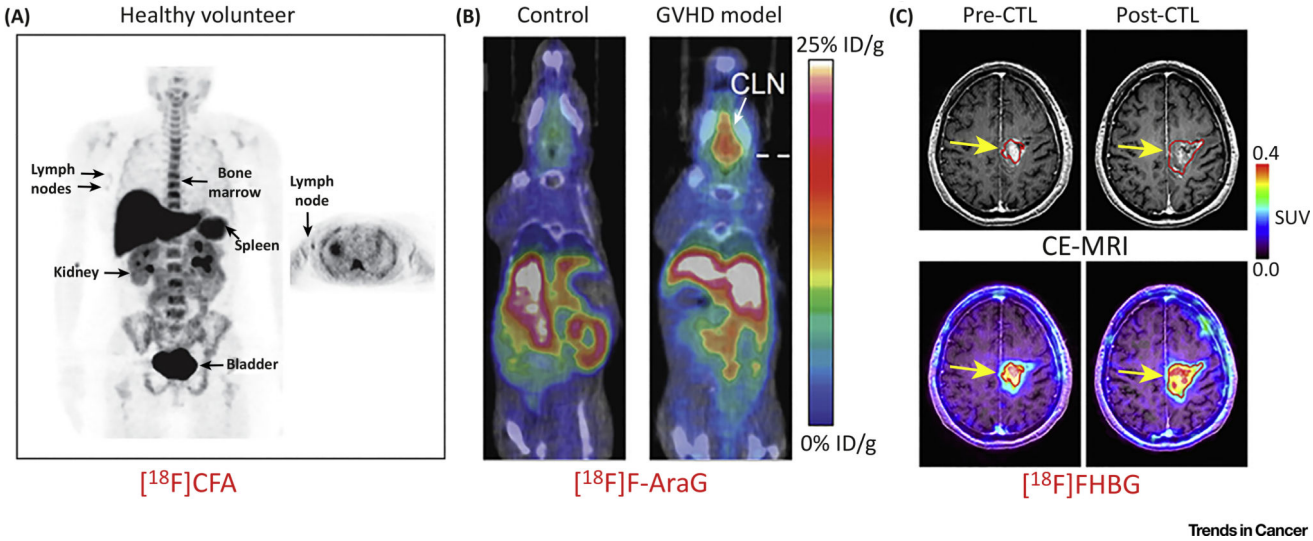

Figure 3. Molecular Imaging of T Cells via Radiolabeled Small Molecules or Positron Emission Tomography (PET) Reporter Probes

(A) A first-in-human study of [^{18}F]CFA, a nucleoside analogue probe, showed significant probe accumulation in deoxycytidine kinase (dCK)-positive tissues (bone marrow, liver, and spleen) and in the axillary lymph nodes of healthy volunteers, indicating its potential to delineate T cells. (B) [^{18}F]F-AraG is an analog of AraG, a compound identified to have specific cytotoxicity toward T lymphocyte and T lymphoblastoid cells versus other immune cell types. [^{18}F]F-AraG PET showed visibly higher tracer uptake in the cervical lymph nodes (CLN) in graft-versus-host disease (GVHD) models. (C) Contrast-enhanced MRI (CE-MRI) and [^{18}F]FHBG PET imaging of recurrent glioma. T1-weighted CE-MRI demonstrated that the tumor size shrank after cytotoxic T cell (CTL) injections (top left panel). Accordingly, the [^{18}F]FHBG signal was significantly increased after CTL infusions, with a 66% increase in total [^{18}F]FHBG activity. Adapted, with permission, from [91,96,109]. Abbreviation: SUV, standardized uptake value.

Table 1

Representative T Cell-Targeting PET Probes[a]

Probe	Target	Radionuclide	Status	Application	Refs
^{64}Cu-DOTA-ipilimumab	CTLA-4	^{64}Cu	Preclinical	TILs	[32]
^{89}Zr-DFO-CD3	CD3	^{89}Zr	Preclinical	TILs	[33]
^{89}Zr-Df-nivolumab	PD-1	^{89}Zr	Clinical trial	TILs	[37–39]
^{89}Zr-Df-pembrolizumab	PD-1	^{89}Zr	Preclinical	TILs	[41]
^{89}Zr-PEG20-X118-VHH	CD8	^{89}Zr	Preclinical	TILs	[57]
^{89}Zr-malDFO-169	CD8	^{89}Zr	Preclinical	TILs	[60]
^{89}Zr-malDFO-GK1.5 cDb	CD4	^{89}Zr	Preclinical	HSCT, IBD	[27,61]
^{89}ZrmalDFO-2.43 cDb	CD8	^{89}Zr	Preclinical	HSCT	[27]
^{89}Zr-Df-IAB22M2C	CD8	^{89}Zr	Clinical trial	TILs	[63]
^{64}Cu-LLP2A	VLA4	^{64}Cu	Preclinical	Tuberculosis	[28]
^{68}Ga-NOTA-GZP	Granzyme B	^{68}Ga	Preclinical	TILs	[69]
[^{18}F]FB-IL-2	IL-2R	^{18}F	Preclinical	TILs	[75]
[^{18}F]FB-IL-2v	IL-2R	^{18}F	Preclinical	TILs	[77]
^{18}F-FLT	Thymidine kinase 1	^{18}F	Clinical	DC vaccine	[86]
[^{18}F]FAC	dCK	^{18}F	Clinical trial	Lymphoid organs	[88]
[^{18}F]CFA	dCK	^{18}F	Clinical trial	TILs	[91,92]
[^{18}F]F-AraG	Deoxyguanosine kinase	^{18}F	Preclinical	GVHD, RA	[96,98]
[^{18}F]FHBG	*HSV1-tk* reporter gene	^{18}F	Clinical trial	CAR-T	[109]
^{89}Zr-aTCRmu-F(ab′)$_2$	TCRmu	^{89}Zr	Preclinical	CAR-T	[111,112]

[a]Abbreviations: CAR-T, chimeric antigen receptor-expressing T cell; DC, dendritic cell; dCK, deoxycytidine kinase; GVHD, graft-versus-host disease; HSCT, hematopoietic stem cell transplantation; IBD, inflammatory bowel disease; IL-2R, interleukin-2 receptors; RA, rheumatoid arthritis; TCRmu, murine T cell receptor beta domain; TIL, tumor-infiltrating lymphocyte; VLA4, very late antigen-4.